Bull. Mater. Sci., Vol. 34, No. 4, July 2011, pp. 873–881. © Indian Academy of Sciences.

Infrared spectra, Raman laser, XRD, DSC/TGA and SEM investigations on the preparations of selenium metal, (Sb_2O_3, Ga_2O_3, SnO and HgO) oxides and lead carbonate with pure grade using acetamide precursors

MOAMEN S REFAT[†,*] and KHALED M ELSABAWY[††]

Department of Chemistry, Faculty of Science, Taif University, 888 Taif, Kingdom of Saudi Arabia
[†]Department of Chemistry, Faculty of Science, Port Said University, Port Said, Egypt
[††]Materials Science Unit, Chemistry Department, Faculty of Science, Tanta University, Tanta 31725, Egypt

MS received 22 April 2010; revised 27 May 2010

Abstract. **Ga_2O_3, Se metal, SnO, Sb_2O_3, HgO and $PbCO_3$ are formed upon the reaction of acetamide aqueous solutions with $Ga(NO_3)_3$, SeO_2, $SnCl_2$, $SbCl_3$, $HgCl_2$ and $Pb(NO_3)_2$, respectively, at 90°C. Different amorphous or crystalline phases can be obtained depending upon the experimental conditions (molar ratios, metal salts and temperature). The chemical mechanisms for the formations of this metal, oxides or carbonate are discussed and the X-ray diffraction, scanning electron microscopy (SEM) and atomic force microscope (AFM) are described. The type of metal ions plays an important role in the decomposition of acetamide, leading to the formation of solid stable (metal, oxides or carbonate), soluble and gases species. These new precursors are more stable preventing the rapid precipitation of metal, oxides or carbonate. Furthermore, this route allows the formation of pure compounds in solutions.**

Keywords. **Oxides; carbonate; XRD; SEM; infrared spectra.**

1. Introduction

Acetamide is used as a plasticizer and in the synthesis of many other organic and inorganic compounds. It is used as a starting material for the synthesis of many applied compounds (Pailloux *et al* 2009; Pollmann *et al* 2009; Zhan *et al* 2009; Ma *et al* 2010). The literature revels that acetamide and its derivatives are forming coordinate bonds with many metal ions at room temperature in aqueous and nonaqueous media through its oxygen (C=O group) or nitrogen atoms (NH_2 group) depending on the type of metal ion used (Paul *et al* 1966; Dunstan 2002; Ağırtaş and Sait Izgi 2009; Chen *et al* 2009). From the chemical viewpoint, the reaction of metal salts with acetamide as a simple organic compound at high temperature has less attention and it is not highlighted in the scientific literature. The nature of the reaction products depend strongly on the type of metal ions and also the metal salt used.

In our previous studies (Nour *et al* 1997; Refat 2004; Refat *et al* 2004a, b; Sadeek *et al* 2004; Teleb *et al* 2004; Sadeek and Refat 2005; Refat and Sadeek 2005; Refat *et al* 2005; Teleb and Refat 2006) concerning the reaction of urea (which contain amido group similar to acetamide) and also simple organic ligand with different metals such as Co(III), Pb(II), Sn(II), Cr(III), Fe(III), Au(III), Sn(IV), V(V) and Mo(IV) at high temperature demonstrate that the types of metal ions beside their anions have a pronounced effect on the nature of the reaction products. The published papers were trended for the reaction of urea with different metal salts at high temperature which lead to identify a novel method for preparation of $pbCO_3$ and $CoCO_3$ (Refat *et al* 2004a), lanthanide carbonates (Refat 2004; Teleb and Refat 2006), limonite, FeO(OH) (Sadeek *et al* 2004), $2ZnCO_3{\cdot}3Zn(OH)_2$ (Sadeek and Refat 2005), $SnOCl_2{\cdot}2H_2O$ (Teleb *et al* 2004), (Cr_2O_3, MnO_2, MoO_3 and WO_3) oxides resulted from a novel oxidation reduction reaction between (K_2CrO_4 or $K_2Cr_2O_7$), $KMnO_4$, Na_2MoO_4 and Na_2WO_4, respectively, with urea in an aqueous solution at ~85°C (Teleb and Refat 2006).

The aim of this publication is to report the synthesis and characterization study of the resulting compounds formed from the reactions of acetamide with $Ga(NO_3)_3$, SeO_2, $SnCl_2$, $SbCl_3$, $HgCl_2$ and $Pb(NO_3)_2$ at high temperature in aqueous media.

2. Experimental

All chemicals used throughout this study were Analar or extra pure grade. The Ga_2O_3, Se metal, SnO, Sb_2O_3, HgO

*Author for correspondence (msrefat@yahoo.com)

and $PbCO_3$ compounds were prepared by mixing equal volumes of aqueous solutions of 0·01 M of $Ga(NO_3)_3$, SeO_2, $SnCl_2$, $SbCl_3$, $HgCl_2$ and $Pb(NO_3)_2$ with 0·1 M of acetamide. The mixtures were heated on a water bath to approximately 90°C for about ~24 h. The precipitate filtered off, washed several times with bidistilled water and dried in *vacuo* over $CaCl_2$. The six-products compounds were received in powder solid form. The elemental analysis for the obtained products shows the absence of carbon and nitrogen elements except for Pb(II) product. The percentage of gallium, selenium, tin, antimony, mercury and lead were determined by gravimetric method in suitable fixed feature.

The infrared spectra of the solid products obtained were recorded from KBr discs using a Shimadzu FT–IR spectrophotometer. The X-ray diffraction patterns for the three compounds under investigation were recorded on Bruker AXS configuration X-ray powder diffraction in National Research Centre, Cairo, Egypt. Samples were scanned on analytical scanning electron microscopy for the Jeol JSM-63OLA and VEECO INNOVA AFM with multi-modes function USA. Raman laser of samples were measured on the Bruker FT Raman with laser 50 mW.

DSC thermograms of the new compounds were obtained on a SCINCO DSC 1500 STA, which was calibrated with indium metal. Sample of 6·40 mg in solid form were placed in aluminum pans with a pierced lid, and heated rate of 10°C min^{-1} under a nitrogen flow. TGA was carried out on a SCINCO TGA 1500 STA apparatus at a heating rate of 10°C min^{-1} under nitrogen atmosphere.

3. Results and discussion

The reaction of aqueous solutions of acetamide with $Ga(NO_3)_3$, SeO_2, $SnCl_2$, $SbCl_3$, $HgCl_2$ and $Pb(NO_3)_2$ produces uncoloured solid products, Ga_2O_3, SnO, Sb_2O_3, HgO and $PbCO_3$ compounds except selenium metal. The formation of these compounds upon the heating of an aqueous mixture of $Ga(NO_3)_3$, SeO_2, $SnCl_2$, $SbCl_3$, $HgCl_2$ and $Pb(NO_3)_2$ with acetamide may be understood as follows

(i) $Ga(NO_3)_3 + CH_3CONH_2 + H_2O \xrightarrow{90^\circ C}$
$Ga_2O_3 + 3HNO_3 + 2CO + NH_3 + 0{\cdot}5H_2$,

(ii) $SeO_2 + CH_3CONH_2 + H_2O \xrightarrow{90^\circ C}$
$Se + 2CO + NH_3 + 2H_2O$,

(iii) $SnCl_2 + CH_3CONH_2 + H_2O \xrightarrow{90^\circ C}$
$SnO + 2CO + NH_3 + 2HCl + H_2$,

(iv) $SbCl_3 + CH_3CONH_2 + H_2O \xrightarrow{90^\circ C}$
$Sb_2O_3 + 3HCl + 2CO + NH_3 + 0{\cdot}5H_2$,

(v) $HgCl_2 + CH_3CONH_2 + H_2O \xrightarrow{90^\circ C}$
$HgO + 2CO + NH_3 + 2HCl + H_2$,

(vi) $Pb(NO_3)_2 + CH_3CONH_2 + 3H_2O \xrightarrow{90^\circ C}$
$PbCO_3 + CO + 2HNO_3 + 9/2H_2$.

From the above six reactions, liberation of different gases (HCl, CO, NH_3 and H_2) and soluble oxidizing products HNO_3 besides different oxide, metal or carbonate solid products occurs during the decomposition of acetamide according to the type of metals and the important role of their metal on the decomposition process via aqueous media.

3.1 *Infrared spectra*

The infrared spectra of the six products are shown in figure 1. Infrared spectra have been widely used as a powerful means of distinguishing between the two possible donation sites of acetamide. A shift in the carbonyl stretching vibration to lower wavenumbers is usually taken to indicate a metal–oxygen bond, while a shift in ν(CO) to higher wavenumbers indicates a metal–nitrogen bond. However, the majority of the evidences indicate that the oxygen atom is the preferred coordination site. The infrared spectra of the obtained products show no bands due to characteristic groups of acetamide (carbonyl and amide groups), but the bands associated to presence of new products observed.

The ν_{as}(CN) of acetamide is observed at around 1400–1500 cm^{-1} (Nakamoto 1978), while, the bending vibration associated with the $-NH_2$ of acetamide is observed as expected as a very strong absorption around 1630 cm^{-1}. The C–N bond symmetric stretching vibration, ν_{as}(CN), is observed at 1000–1100 cm^{-1} for acetamide. The rocking, twisting and wagging modes associated with the $-NH_2$ group are observed around 900 cm^{-1}. The bending motions δ(NCO) is observed in the spectrum of acetamide near to 600 cm^{-1}. The assignments of these bands are due to free acetamide ligand, these bands are absent in the spectra of the three new compounds with appearing new bands.

For the Ga_2O_3, SnO, Sb_2O_3 and HgO compounds, there are many bands (Ga_2O_3 = 1132, 885, 571, 514 and 451 cm^{-1}; SnO = 1044, 929, 610 and 504 cm^{-1}; Sb_2O_3 = 839, 772, 689, 608, 506, 477 and 451 cm^{-1}; HgO = 1177, 1038, 922, 495, 469 and 440 cm^{-1}) refer to the stretching vibration motions of the ν(M–O). The OH stretching motions of the H_2O molecule are observed in its expected region at 3450–3530 cm^{-1}. Although it is difficult to differentiate between H_2O molecule and –OH group, the former is associated with other modes such as rocking, twisting and ν(M–O) vibrations. The bands observed at 900, 700 and 400–500 cm^{-1} can be assigned to these motions, respectively (Nakamoto 1978).

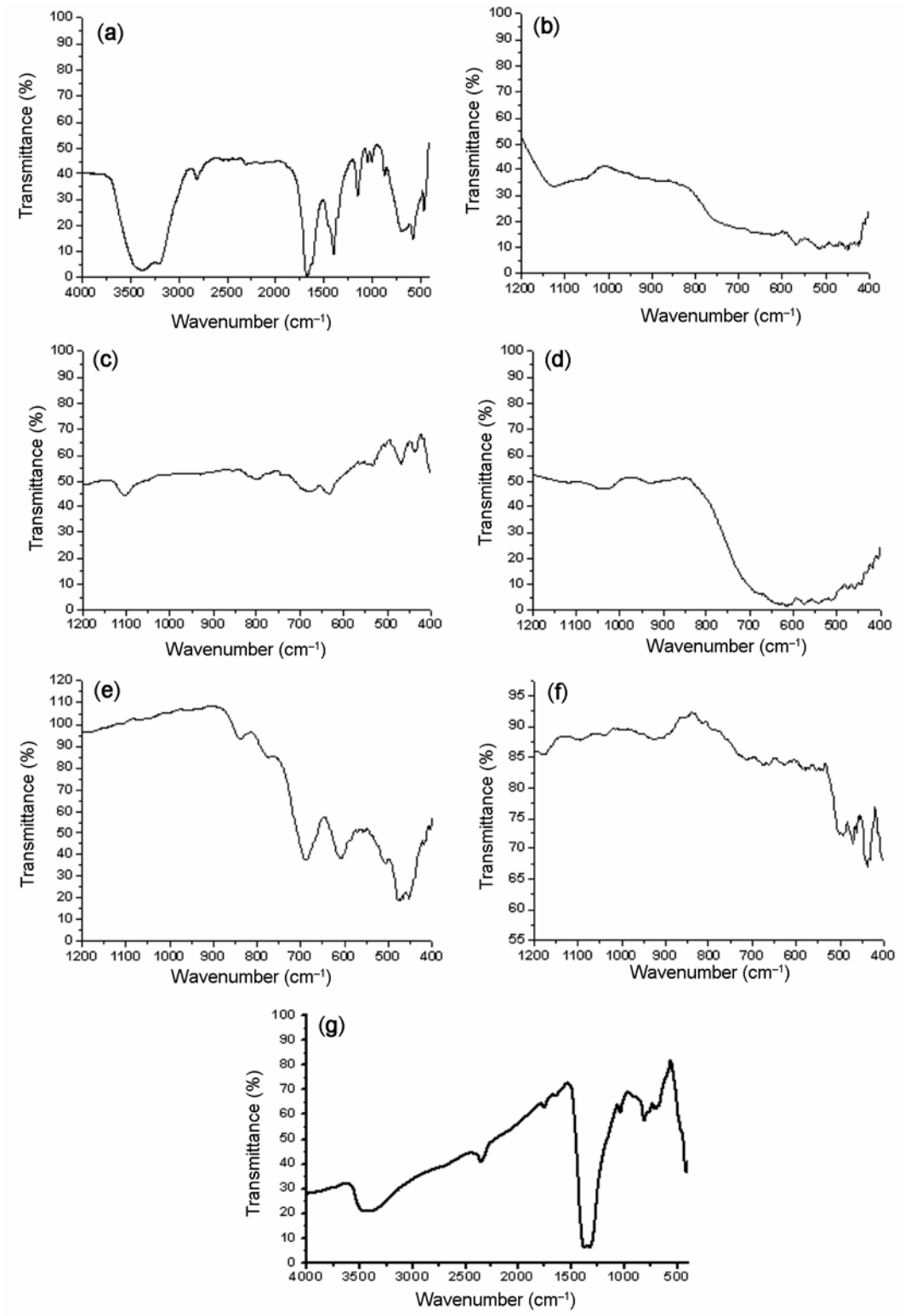

Figure 1. Infrared spectra of (**a**) acetamide as a free ligand, (**b**) Ga_2O_3, (**c**) Se metal, (**d**) SnO, (**e**) Sb_2O_3, (**f**) HgO and (**g**) $PbCO_3$ compounds.

Finally, the infrared spectrum of $PbCO_3$ compound can be attributed to formed CO_3^{2-} ion in planar geometry, and therefore belongs to the D_{3h} symmetry. It is expected to display four modes of vibrations, $A_1' + A_2'' + 2E'$ (E' is a doubly degenerate motion). The vibration A_1' is only Raman-active, while the other ν_2, ν_3 and ν_4 are infrared-active. The stretching vibrations of the type, ν(C–O); $\nu_3(E')$ is observed as a strong broad band at 1388 cm^{-1}

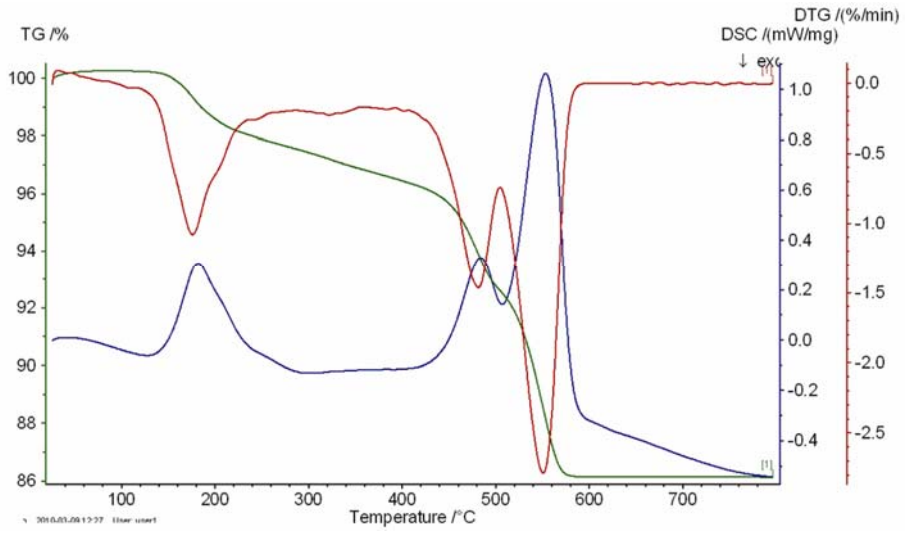

Figure 2. TG/DTG/DSC curve of $PbCO_3$ compound.

while the stretching vibration ν(C–O); $\nu_1(A_1')$ is observed in the region ~1030 cm^{-1} as a medium-to-weak band. It should be indicated here that this motion (A_1') should be infrared inactive, its weak appearance in the spectrum of $MCO_3{\cdot}nH_2O$ could be related to weak solid–solid interactions causing the symmetry of CO_3^{2-} to be lowered than D_{3h}. The out-of-plane of vibration, δ(OCO), $\nu_2(A_2'')$ is observed in the range of ~822 cm^{-1} as a medium strong band, while the angle deformation bending vibration δ(OCO), $\nu_4(E')$ appear at 714 cm^{-1} as a medium weak. The infrared spectra of Pb(II) carbonate, $PbCO_3{\cdot}nH_2O$, show that some of these products clearly have an uncoordinated water. The band related to the stretching vibration ν(O–H) of uncoordinated H_2O is observed as expected in the range of ~3000 cm^{-1}.

3.2 *Thermal analysis TG–DTG*

The TG/DSC curve of $PbCO_3$ compound is shown in figure 2. Synthetic lead carbonate was prepared from interaction of lead(II) nitrate and acetamide in aqueous media at high temperature and subjected to thermal analysis studies. The decomposition product was subjected to infrared analysis and was found to be a Pb_2O_3. From the TG/DSC plot of synthetic $PbCO_3$ seen in figure 3 there is a large sequential mass loss equating to approximately 13·70% of the total mass. The combined large mass loss started at 160°C and was complete by 580°C. There was no evidence in the accompanying curves of water; this confirmed that water did not exist in the sample. The theoretical decomposition reaction for synthetic $PbCO_3$ is as follows

$$2PbCO_{3(s)} \rightarrow Pb_2O_{3(s)} + CO_{2(g)} + CO_{(g)}.$$

The expected mass loss should be equivalent to 13·50% of the total mass, the analysis resulted in an actual mass loss of 13·70% overall mass loss which is very close to that of the theoretical calculated percentage loss.

3.3 *Phase identification and XRD spectra*

The XRD patterns of Ga_2O_3, Se metal and Sb_2O_3 are shown in figures 3a–c. All detectable peaks of Ga_2O_3, Se metal and Sb_2O_3 are indexed as Ga_2O_3, Se metal and Sb_2O_3 structures, which are matched and compared with the ASTM standard cards and ICSD-data bank (Karlesruhe-Germany).

As clear in figure 3a–c the dominating phases for selenium metal, gallium oxide and antimony oxide that assigned by S, G and A-letters are found to be typical to the single crystal data recorded in ICSD-data bank for those oxides.

Many investigators (Barber and Menke 1984; Boris 1999; DeCamps *et al* 1972; Bonnhomme *et al* 1993; *Elsabawy et al* 2009; Elsabawy 2009) studied the applications of these oxides as individual, binary and ternary mixed system in catalysis, photochemical degradation and environmental issues due to their huge surface area and cations centres existed on its surface layers. From this point of view, others (Boris 1999; DeCamps *et al* 1972) investigated more complicated systems such as binding of oxides with polymeric materials or organic substrates to increase or promote the catalytic activity of these materials. Confirmation of synthesized oxides structures were performed through theoretical treatment by visualizing of structures of both (HgO and SnO) as model of synthesized materials via Diamond Impact Crystal Molecular Structure Version 3.2-Visulizer.

Figures 3d–e display the experimental XRD recorded for samples (HgO and SnO) in the range (2θ = 10–30°) the red circles and blue arrows are as follows.

The indexed assignments for each mercuric and tin oxides phases, while figure 4 shows the visualized XRD-constructed for mercuric oxides. The matching and comparison between XRD-profile of experimental data and visualized XRD-profile data indicated that synthesized HgO was nearly identical with visualized structure with ratio higher than 85%. Figure 6 describes the high resolution zoom in zone of experimental XRD-profile recorded in the specific range ($2\theta = 60–70°$) which compared with the same region in figure 4 was observed that the principal three lines located in figure 4 are present nearly in the same positions in figure 5 with some more extra peaks due to impurity phases in minor.

Figures 5a, b are the molecular structures drawn for HgO and SnO depending up on the crystal structure data evaluated from experimental XRD of both HgO and SnO oxides in which HgO crystallized in orthorhombic phase with Imm2 space group and lattice parameters $a = 3{\cdot}3113$, $b = 3{\cdot}5288$ and $c = 3{\cdot}688$ Å, while SnO crystallized in tetragonal unit cell with $P4/nmms$ space group. A visualization study made is concerned by matching and comparison of calculated theoretical data as bond distances, oxidation states and bond torsion on the crystal structure formed. The study exhibited good fitting between experimental and theoretical data.

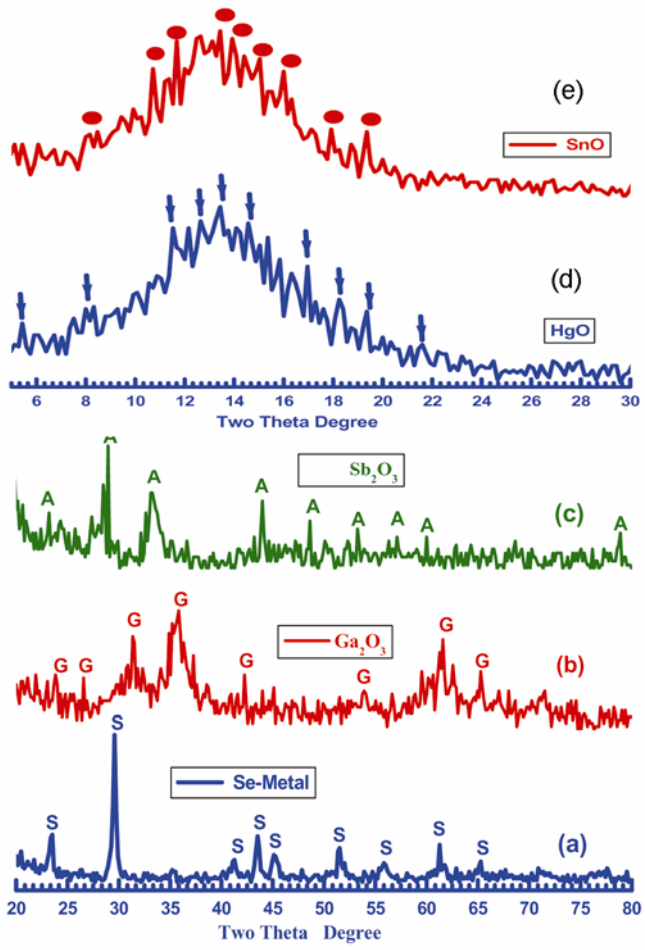

Figure 3a–e. X-ray diffraction patterns recorded for (a) Se metal (b) Ga_2O_3 and (c) Sb_2O_3 compounds. X-ray diffraction patterns recorded for (d) SnO and (e) HgO.

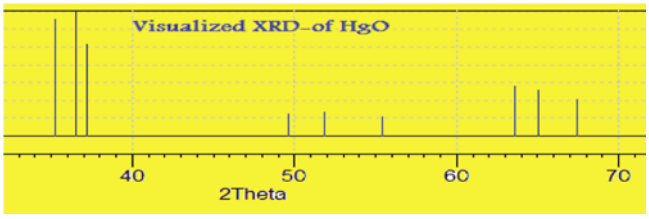

Figure 4. Visualized XRD of HgO prepared via acetamide precursor.

3.4 *Scanning electron and atomic force microscopy*

The SEM micrographs of the prepared Ga_2O_3, Se, SnO, Sb_2O_3, HgO and $PbCO_3$ compounds are shown in figure 6. The average grain size were calculated and found in between 2·75 μm for Ge_2O_3, 0·65 μm for selenium metal, 0·9 μm for tin oxide (SnO), 2·2 μm for Sb_2O_3, 0·85 μm for mercuric oxide and finally 2·3 μm for lead carbonate sample, respectively. The EDX examinations for random spots in the same sample confirmed and are consistent with our XRD analysis. From figure 6 it is difficult to observe inhomogeneity within the same micrograph due to the solution route synthesis with acetamide precursor and is very fine and the particle size must be in nano-

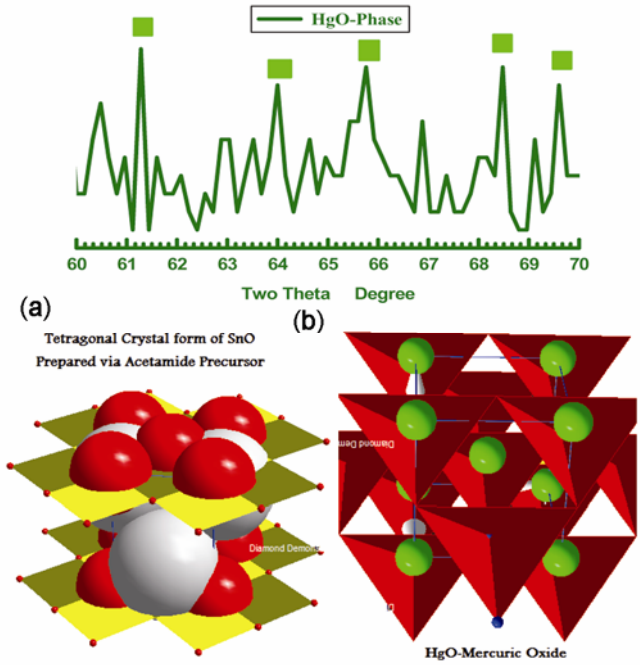

Figure 5. High resolution XRD recorded for HgO-oxide. (**a**) Tetragonal molecular structure of SnO and (**b**) orthohombic molecular structure of HgO.

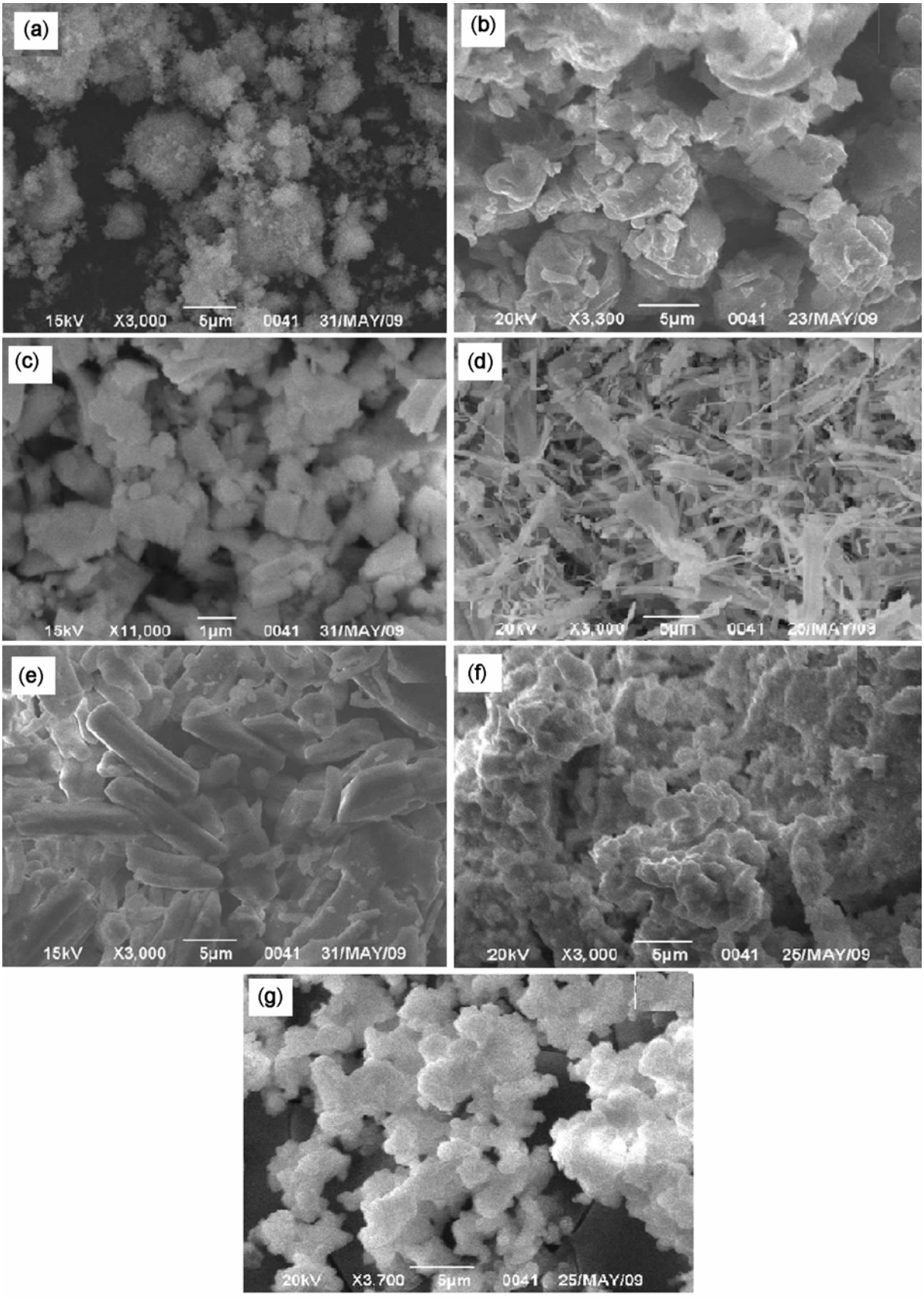

Figure 6. SEM micrographs of (**a**) acetamide as a free ligand, (**b**) Ga_2O_3, (**c**) Se metal, (**d**) SnO, (**e**) Sb_2O_3, (**f**) HgO and (**g**) $PbCO_3$ compounds.

range specially for selenium-metal and mercuric oxide samples. The grain size for nano-oxides were calculated according to 'Scherrer's formula' (Scherrer 1918; Vanderzee *et al* 1974; Li *et al* 1997; Jenkins and Snyder 1996; Locha *et al* 2002)

$$B = 0{\cdot}87\lambda/D\cos\theta,$$

where D is the crystalline grain size in nm, θ is half of the diffraction angle in degree, λ the wavelength of X-ray source (Cu-K_α) in nm, and B is degree of widening of diffraction peak which is equal to the difference of full width at half maximum (FWHM) of the peak at the same diffraction angle between the measured sample and standard one.

From SEM-maping, the estimated average grain size was found to be lower than those calculated applying Scherrer's formula for the same compounds. This indicates that the actual grain size in the material bulk is smaller than that detected on the surface morophology. Similar behaviour of grains size calculations differences between bulk and material surface was recorded by many authors (Sekkina and Elsabawy 2002; Sekkina *et al* 2004; Elsabawy 2005) due to ambient processing temperature and applied experimental condition.

Figure 7 shows the variation of calculated grain size from SE-micrograph according to ionic size of each synthesized oxides of reactant materials. Synthesized oxides were arranged according to the sequences as is clear in figure 7 with minimum grain size 0·65 μm for selenium metal and maximum 2·75 μm for gallium oxide. Many researchers (Fayette *et al* 2000; Tschöpe 2001; Pérez 2002) reported that grain size can be affected by many parameters such as reactant counter ions and grain orientations that could make a noticeable change in the physical properties of synthesized product as thermal, ionic conductivity and corrosion behaviour (Pérez 2002).

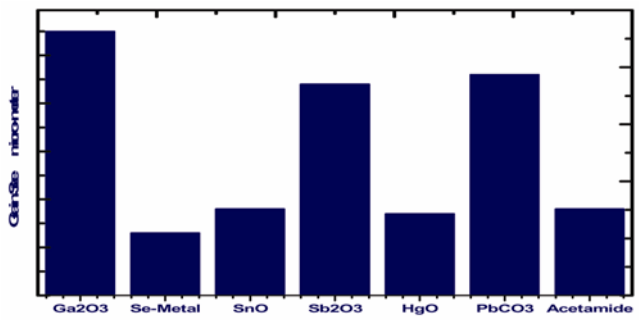

Figure 7. Synthesized compounds versus calculated grain size.

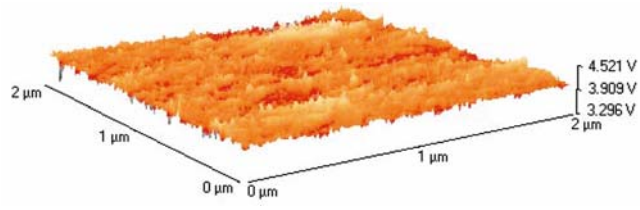

Figure 8. 3D-AFM-tapping mode imaging captured for Se-metal prepared via acetamide precursor.

For accurate particle size calculations and morphological properties of selenium surface, AFM-microscopy tapping mode was applied on the solid pellet of selenium metal as model of different yields produced through ignition of metal-acetamide precursors to evaluate nanometric features of the resultant materials.

Figure 8 shows the three-dimensional image for selenium-metal through tapping mode; it was observed that movement of the tip through the z-axis not similar which means that the up and down zones of the surface is not homogeneous through the scanned area which is too small (2 × 2 μm).

The analysis of the SEM images and AFM shown in figure 9 indicate that the average particle size for selenium sample is between 15–35 nm which confirm that acetamide synthesis technique yields to nano-product.

Peng *et al* (2007) reported that 36 nm of Se metal has lower toxicity than selenite or selenomethionine with higher particle sizes, but all of these forms of (Se) possess similar ability to increase selenoenzyme levels. They deduced also that the size of nanoparticles play an important role in their biological activity: as expected, from range 5–200 nm for Se which can be directly scavenge free radicals *in vitro* in a size-dependent fashion. Accordingly the present techniques of synthesizing selenium metal within the range 15–35 nm is a unique and pioneer technique to increase the validity for selenium in biological reaction and leading new trends to decrease toxicity of selenium of higher particle size as reported in (Peng *et al* 2007).

3.5 *Raman laser spectra*

The Raman laser spectra of the six compounds were recorded and assigned. The Raman spectrum of the

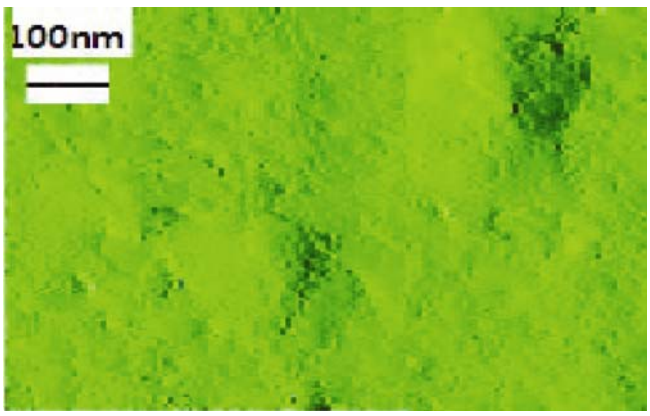

Figure 9. AFM-image captured for selenium-metal surface.

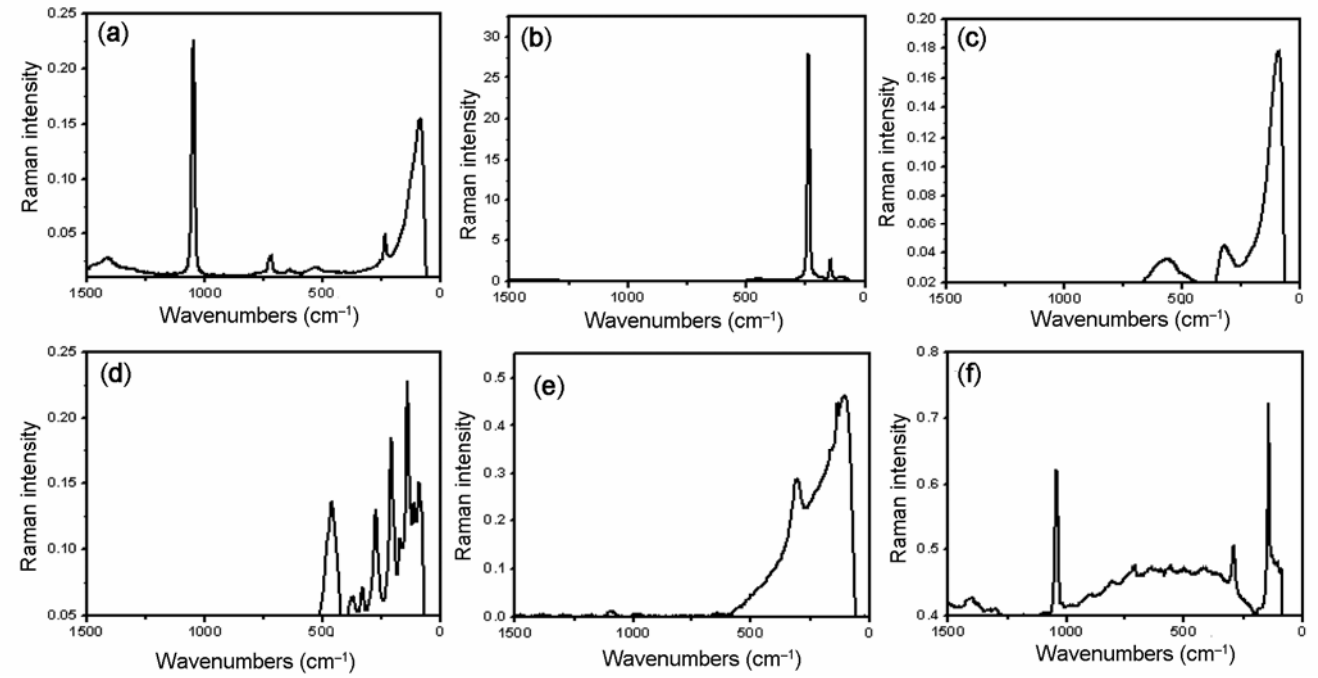

Figure 10. Raman spectra of (**a**) acetamide as a free ligand, (**b**) Ga_2O_3, (**c**) Se metal, (**d**) SnO, (**e**) Sb_2O_3, (**f**) HgO and (**g**) $PbCO_3$ compounds.

acetamide, Ga_2O_3, Se, SnO, Sb_2O_3, HgO and $PbCO_3$ compounds are shown in figures 8a–f. Raman spectrum of the Ga_2O_3 is shown in figure 8a. The band at 717 cm^{-1} is assigned to the ν_1 symmetric stretching bands of Ga–O units. The band at 643 cm^{-1} is assigned to O–Ga–O bending modes of the Ga_2O_3 units. According to Gao *et al* (2002) and Rao *et al* (2005) the wavenumbers of Ga_2O_3 materials found Raman bands at 160, 194, 332, 409, 641 and 742 cm^{-1}. The results of both these papers are matched with the data in this paper. The Raman bands reported in this study are at 237, 528, 643 and 717 cm^{-1}.

The Raman spectrum of Se metal is reported in figure 8b. For the pure selenium sample, the spectrum is characterized by a strong band at 237 cm^{-1} which is attributed to the vibrational mode of –Se–Se–Se– chains (40, 41). Additional weaker features can be revealed at 141 cm^{-1} which are assigned to the presence of Se_8 rings and to the bending modes of Se units (Kovanda *et al* 2003; Iovu *et al* 2005).

Figure 8c shows Raman spectra of SnO within frequency range (0·0–1500 cm^{-1}). The Raman spectrum of pure SnO show the same behaviour of ZnO which shows several bands which include 565 and 324 cm^{-1}. The most intense band can be seen at 565 cm^{-1} (Mikla 1997; Wang *et al* 2004), as shown in figure 8c, which confirm the presence of SnO in pure form. Sb_2O_3 Raman spectrum (figure 8d) contains several bands at 457, 369, 328, 270, 209 and 141 cm^{-1} which are assigned to Sb–O stretching and O–Sb–O bending motions. These identical bands are in good agreement with data in literature (Cody *et al* 1979; Mestl *et al* 1994; Terashima *et al* 1996). The Raman spectrum of the HgO is represented in figure 8e with clearly obvious two detectable bands at 311 and 135 cm^{-1} due to Hg–O stretching frequency. Under ambient conditions, lead carbonate ($PbCO_3$) have 30 Raman active ($9A_{1g} + 6B_{1g} + 6B_{2g} + 9B_{3g}$) and 18 IR active ($8B_{1u} + 5B_{2u} + 5B_{3u}$) vibrational modes. We observed 14 Raman modes in the range 100–1600 cm^{-1}, in good agreement with the findings of Lin and Liu (1997). These modes can be divided into four main regions as follows:

646 cm^{-1}	$B_{3g} + A_{1g} + B_{2g} + B_{1g}$
707 cm^{-1}	(ν_4-in-plane band of CO_3 group)
809 + 907 cm^{-1}	A_{1g} (ν_2-out-of-plane band of CO_3 group)
1046 cm^{-1}	A_{1g} (ν_1-symmetric C–O stretching of CO_3 groups)
1399 + 1303 cm^{-1}	A_{1g} (ν_3-asymmetric C–O stretching of CO_3 groups)

4. Conclusions

The available experimental work suggest that the acetamide compound play an important role as precursor in the preparation of Ga_2O_3, selenium metal, SnO, Sb_2O_3, HgO and $PbCO_3$ compounds. The types of metals and metal salts also have the significant effect on the decomposition process of acetamide in aqueous media. Different tools of analyses are used in the interpretative of the resulted compounds like infrared and Raman spectra,

thermal analysis, XRD and scanning electron microscopy.

References

Ağırtaş M S and Sait Izgi M 2009 *J. Mol. Struct.* **927** 126

Barber T E and Menke R D 1984 *The Am. J. Emergency Med.* **2** 500

Bonnhomme C, Henryand M and Livage J 1993 *J. Non-Cryst. Solids* **159** 22

Boris L'vov V 1999 *Thermochim. Acta* **333** 21

Chen S -C, Hsueh H -H, Chen C -H, Lee C S, Liu F -C, Lin I J B, Lee G H and Peng S -M 2009 *Inorg. Chim. Acta* **362** 3343

Cody C A, DiCarlo L and Darlington R K 1979 *Inorg. Chem.* **18** 1572

DeCamps E A, Durand M, Marqueton Y and Ayrault B 1972 *Optics Commun.* **4** 358

Dunstan P O 2002 *Thermochim. Acta* **389** 25

Elsabawy K M 2005 *Physica C* **432** 263

Elsabawy K M 2009 *Mens Agitate* **4** (in press)

Elsabawy K M, Sekkina M M and Bediwy M M 2009 *Int. J. Pure & Appl. Chem.* **4** 265

Fayette S, Smith D S, Smith A and Martin C 2000 *J. Eur. Ceramic Soc.* **20** 297

Gao Y H, Bando Y, Sato T, Zhang Y F and Gao X Q 2002 *Appl. Phy. Lett.* **81** 2267

Iovu M S, Kamitsos E I, Varsamis C P E, Boolchand P and Popescu M 2005 *Chalcogenide Lett.* **2** 21

Jenkins R and Snyder R L 1996 *Introduction to X-ray powder diffractometry* (John Wiley & Sons Inc) pp 89–91

Kovanda V, Vlček M and Jain H 2003 *J. Non-Cryst. Solids* **326&327** 88

Li Q, Yuan X, Zeng G and Xi S 1997 *Mat. Chem. & Phys.* **47** 239

Lin C C and Liu L G 1997 *J. Phys. Chem. Sol.* **58** 977

Locha V, Machek J and Tichý J 2002 *Appl. Catalysis* **A228** 95

Ma Z, Han S, Kravtsov V C and Moulton B 2010 *Inorg. Chim. Acta* **363** 387

Mestl G, Ruiz P, Delmon B and Knözinger H 1994 *J. Phys. Chem.* **98** 11276

Mikla V I 1997 *J. Phys., Condens. Matter.* **9** 9209

Nakamoto K 1978 *Infrared and Raman spectra of inorganic and coordination compounds* (New York: Wiley Interscience) 3rd edn

Nour E M, Teleb S M, Al-Khososy N A and Refat M S 1997 *Synth. React. Inorg. Met-Org. Chem.* **27** 505

Pailloux S, Binyamin I, Deck L M, Hay B P, Duesler E N, Zakharov L N, Kassel W S, Rheingold A L and Paine R T 2009 *Polyhedron* **28** 3979

Paul R C, Sreenathan B R and Chadha S L 1966 *J. Inorg. Nucl. Chem.* **28** 1225

Peng D, Zhang J, Liu Q and Taylor E W 2007 *J. Inorg. Biochem.* **101** 1457

Pérez P 2002 *Corrosion Sci.* **44** 1793

Pollmann S, Düchting P and Weiler E W 2009 *Phytochemistry* **70** 523

Rao R, Rao A M, Xu B, Dong J, Sharma S and Sunkara M K 2005 *J. Appl. Phys.* **98** 943

Refat M S 2004 *Synth. React. Inorg. Met.-Org. Chem.* **34** 1605

Refat M S and Sadeek S A 2005 *Latvian J. Chem.* **4** 343

Refat M S, Sadeek S A and Nasr D E 2005 *Bull. Chem. Technolog. Maced.* **24** 153

Refat M S, Sadeek S A and Teleb S M 2004a *J. Argen. Chem. Soc.* **92** 23

Refat M S, Teleb S M and Sadeek S A 2004b *Spectrochim. Acta* **A60** 2803

Sadeek S A and Refat M S 2005 *J. Coord. Chem.* **58** 1727

Sadeek S A, Refat M S and Teleb S M 2004 *J. Korea, Chem. Soc.* **48** 358

Scherrer P 1918 *Göttinger Nachrichten Gesell.* **2** 98

Sekkina M M A and Elsabawy K M 2002 *Solid State Commun.* **123** 1

Sekkina M M A, Eldaly H A and Elsabawy K M 2004 *Supercond. Sci. Technol.* **17** 93

Teleb S M and Refat M S 2006 *Bull. Chem. Technolog. Maced.* **25** 57

Teleb S M, Refat M S and Sadeek S A 2004 *Ukrainian Chem. J.* **68** 35

Terashima K, Hashimoto T, Uchino T, Kim S -H and Yoko T 1996 *J. Ceram. Soc. Japan* **104** 1008

Tschöpe A 2001 *Solid State Ionics* **139** 267

Vanderzee C E, Rodenburg M L N and Berg R L 1974 *J. Chem. Thermodynamics* **6** 17

Wang R P, Xu G and Jin P 2004 *Phys. Rev. B: Condens. Matter Mater. Phys.* **69** 113303

Zhan P, Liu X, Fang Z, Li Z, Pannecouque C and De Clercq E 2009 *Eur. J. Med. Chem.* **44** 4648